

YALE PEABODY MUSEUM

P.O. BOX 208118 | NEW HAVEN CT 06520-8118 USA | PEABODY.YALE. EDU

JOURNAL OF MARINE RESEARCH

The *Journal of Marine Research*, one of the oldest journals in American marine science, published important peer-reviewed original research on a broad array of topics in physical, biological, and chemical oceanography vital to the academic oceanographic community in the long and rich tradition of the Sears Foundation for Marine Research at Yale University.

An archive of all issues from 1937 to 2021 (Volume 1–79) are available through EliScholar, a digital platform for scholarly publishing provided by Yale University Library at <https://elischolar.library.yale.edu/>.

Requests for permission to clear rights for use of this content should be directed to the authors, their estates, or other representatives. The *Journal of Marine Research* has no contact information beyond the affiliations listed in the published articles. We ask that you provide attribution to the *Journal of Marine Research*.

Yale University provides access to these materials for educational and research purposes only. Copyright or other proprietary rights to content contained in this document may be held by individuals or entities other than, or in addition to, Yale University. You are solely responsible for determining the ownership of the copyright, and for obtaining permission for your intended use. Yale University makes no warranty that your distribution, reproduction, or other use of these materials will not infringe the rights of third parties.



This work is licensed under a Creative Commons Attribution-NonCommercial-ShareAlike 4.0 International License.
<https://creativecommons.org/licenses/by-nc-sa/4.0/>



A theory of the wind-driven circulation II. Gyres with western boundary layers

by William R. Young^{1, 2} and Peter B. Rhines¹

ABSTRACT

The quasigeostrophic, wind-driven circulation theory given by Rhines and Young (1982b) is extended in two directions.

First, we consider forcing patterns which are not contrived so as to close without a western boundary layer. The resulting barotropic circulation pattern (see Fig. 1) has the well known east-west asymmetry produced by the β -effect. Our goal is to present a thorough description of the associated density field and baroclinic currents as predicted by the theory of Rhines and Young (1982b).

Secondly, we consider the problem of closing the circulation by appending western boundary layers. We argue that in the southern region, where fluid enters the boundary layer from the Sverdrup interior, an inertial boundary layer forms. In the northern region, where fluid leaves the boundary layer, there is a damped, stationary, baroclinic Rossby wave which provides the dissipation required to balance the forcing. This wave is neutrally stable according to the Charney-Stern criterion for baroclinic instability and the flow is suggestive of finite amplitude baroclinic instability in which the disturbance has equilibrated by reducing the supercriticality of the mean flow.

Estimates of the depth to which the wind gyre penetrates (of order $(f/N)(U/\beta)^{1/2}$ where f is Coriolis frequency, N buoyancy frequency, U the mean velocity and β the northward gradient of f) are improved using variable N , and accord reasonably well with observations, including the apparently greater depth penetration of the gyre in the Pacific, as compared with the Atlantic.

1. Introduction

Recently Rhines and Young (1982a,b) (RYa and RYb hereafter) have developed an analytic theory of the wind-driven circulation in which the key ingredients are:

- (i) the production of closed geostrophic contours in subsurface density layers if the external forcing (i.e., the Ekman pumping) is sufficiently strong.
- (ii) the nonuniqueness of the flow in these closed regions of dissipation is entirely neglected.

1. Woods Hole Oceanographic Institution, Woods Hole, Massachusetts, 02543, U.S.A.

2. Present address: Marine Physical Laboratory A005, Scripps Institution of Oceanography, San Diego, California, 92152

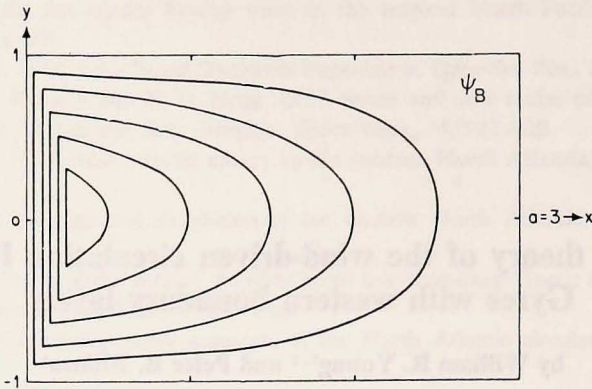


Figure 1. The barotropic streamfunction given by (2.6a). The western boundary layer is shown schematically.

- (iii) the selection of a unique solution by weak dissipation and the calculation of the flow by an extension of the Batchelor-Prandtl theorem.
- (iv) the homogenization of potential vorticity in subsurface density layers if the dominant dissipative mechanism is lateral diffusivity of potential vorticity, due to say mesoscale eddies.

This last theoretical prediction is supported by both ocean observations (Coats, 1981; McDowell *et al.*, 1982) and numerical experiments (Holland, 1982; McWilliams and Chow, 1981; and Bleck and Boudra, 1981). In RYb simple circulation patterns were calculated using the ideas above. Attention was restricted to "mid-ocean" gyres in which it was assumed that the Ekman pumping w_E satisfied the condition:

$$\int_{-\infty}^{\infty} w_E(x', y) dx' = 0. \quad (1.1)$$

The above ensures that the barotropic streamlines calculated from the Sverdrup relation:

$$H\psi_B = -f_0\beta^{-1} \int_a^{\infty} w_E(x', y) dx' \quad (1.2)^3$$

close naturally so that it is not necessary to consider western boundary layer dynamics.

In this note the theory given by RYa and b will be extended in two directions. First, we will consider models of w_E which do not satisfy (1.1). This naturally leads to the second extension: the closure of the circulation by appending a western

3. In (1.2) ψ_B is the barotropic streamfunction. In a quasigeostrophic layered model, if ψ_i and H_i are the streamfunction and layer thickness of the i 'th layer then $H\psi_B = \sum_i H_i \psi_i$ and $H = \sum H_i$. β is the north-south gradient of the vertical component of the Coriolis vector: $f = f_0 + \beta y$ on a β -plane.

boundary layer. This is of course the same problem which arises in homogeneous circulation theory. In the baroclinic theories discussed here all the familiar difficulties of the homogeneous theory re-emerge, compounded by the addition of an extra spatial dimension.

In sections 2 and 3 we begin by calculating the circulation in the Sverdrup interior, away from the western boundary layer. In subsurface density layers the fluid is either motionless or has uniform potential vorticity. This is used to calculate both the extent of the homogenized region and the three dimensional structure of the wind-driven flow within it. The flow satisfies the Sverdrup constraint on the vertically integrated transport and exhibits many realistic features such as the poleward migration of gyre centers with depth.

The quasigeostrophic approximation is used throughout this note and the calculation of the flow in the Sverdrup interior is similar to that in RYb. In section 2 the density structure is approximated by a "2 1/2-layer" model (two active layers over a deep, quiescent layer) while in section 3 we increase the vertical resolution by using a continuously stratified model.

In section 4 boundary layer dynamics are considered for the first time. One of the most unsatisfactory aspects of homogeneous circulation theory is the parameterization of dissipation in the western boundary layer. This is unavoidable since it is necessary to include some form of dissipation (i.e. an eddy viscosity) to remove the vorticity put into the fluid by the wind stress. Perhaps the most sophisticated analytic example of this is Moore's (1963) damped stationary Rossby wave which is confined to the northwest corner of the basin and acts as a set of baffles to give the vorticity sufficient time to diffuse out of the basin (Pedlosky, 1979, section 5.10). Thus although this model, and the simpler ones due to Stommel (1948) and Munk (1950), are internally consistent, they are open to criticism because the structure of the western boundary layer depends strongly on how the smaller scale processes are parameterized. Fortunately the principal conclusion, viz. the boundary layer is on the west, requires only that the eddy viscosities be positive!

Now, in the upper layer of a multilayer model the considerations in the previous paragraph are directly relevant. There is strong vorticity source of one sign, w_E , and so dissipation must be important on every streamline.

The boundary layer closure we adopt is a two-layer version of Moore's (1963) calculation in which this dissipation is provided by a damped stationary baroclinic Rossby wave in the northwest corner of the basin. The novelty is that in the lower layer this wave exists on a mean flow which has uniform potential vorticity. Thus the wave is neutrally stable according to the Charney-Stern criterion for baroclinic instability. Consequently there are no potential vorticity perturbations associated with the wave in the lower layer. The entire configuration is reminiscent of a wave generated by baroclinic instability which equilibrates by erasing the supercriticality of the mean flow (e.g., Pedlosky, 1970, 1971 and 1972).

2. The Sverdrup interior: the two and a half layer model

a. The three layer quasigeostrophic equations. Throughout this article we use the quasigeostrophic equations in which the thickness of an isopycnal layer is linearized about its mean value. Consider then a three layer model in which the thickness of the lowest layer is much greater than that of the other two:

$$H_3 \gg H_1, H_2 .$$

This ensures that the displacement of the lowest interface cannot produce fractional depth changes comparable to the β -effect in the lowest layer. Thus away from inertial boundary layers the lower layer potential vorticity, q_3 , is dominated by the β -effect:

$$q_3 \cong \beta y$$

and so all the geostrophic contours in the lowest layer are blocked by coastal boundaries. This implies that the flow in the lowest layer is weak, since weak vertical stresses produce only weak flow across *blocked* contours (Rhines and Holland, 1979). According to this reasoning then, a negligible fraction of the Sverdrup transport is in the lowest layer and

$$H\psi_B \cong H_1 \psi_1 + H_2 \psi_2 . \quad (2.1)$$

The assumption that the lower layer is motionless reduces the three layer model to an equivalent two layer model. The boundary layer analysis in this article is also based on this two layer model. It is important to realize that the two layers represent the upper thermocline waters rather than the complete column.

The three layer quasigeostrophic equations, with $\psi_3 = 0$, are then

$$J(\psi_1, q_1) = (f_0 w_B / H_1) + (\text{dissipation}) \quad (2.2a)$$

$$J(\psi_2, q_2) = (\text{dissipation}) \quad (2.2b)$$

where the potential vorticities are

$$q_1 = f + \nabla^2 \psi_1 + (f_0^2 / g' H_1) (\psi_2 - \psi_1) \quad (2.3a)$$

$$q_2 = f + \nabla^2 \psi_2 + (f_0^2 / g' H_2) (\psi_1 - \psi_2) + (f_0^2 / g'' H_2) (-\psi_2) \quad (2.3b)$$

and

$$f = f_0 + \beta y$$

is the Coriolis frequency. The reduced gravities are:

$$g' = g \left(\frac{\rho_2 - \rho_1}{\rho_0} \right) \text{ and } g'' = g \left(\frac{\rho_3 - \rho_2}{\rho_0} \right) .$$

Simple scale estimates show that in the Sverdrup interior of a wind-driven gyre

the relative vorticity is negligible in (2.3). Suppose for instance that the horizontal length scale is $L \cong 10^8$ cm and a typical horizontal velocity is $U \cong 1$ cm s⁻¹. Then

$$\frac{\beta y}{\nabla^2 \psi} \cong \frac{\beta L^2}{U} \cong 10^3$$

so that the relative vorticity may be neglected in the interior. On the other hand if the geostrophic contours are to close, the vortex stretching terms in (2.3) must be comparable in magnitude to the β -effect. This observation is used in the next section to obtain simple estimates of the vertical length scale and the horizontal velocity scale of the wind-driven flow in terms of external variables such as β and w_E .

For simplicity we will assume

$$g' = g'' \text{ and } H_1 = H_2$$

and define:

$$F = f_0^2/g'H_1 = \{\text{Rossby radius of deformation}\}^{-2}.$$

b. The Sverdrup constraint. The Sverdrup constraint is obtained by forming the sum H_1 (2.2a) + H_1 (2.2b) and neglecting the dissipation. Note how the large nonlinear vortex stretching terms vanish leaving

$$\beta H \psi_{Bx} = f_0 w_E$$

where

$$H_1(\psi_1 + \psi_2) = H \psi_B. \quad (2.4)$$

The barotropic streamfunction in the interior is now obtained by integrating (2.4) from x to the eastern boundary, $x = a$, where $\psi_B = 0$. One obtains

$$\begin{aligned} \beta H \psi_B &= -f_0 \int_x^a w_E dx' \\ &= -f_0(a-x) w_E(y) \end{aligned} \quad (2.5)$$

if w_E is independent of x . In this article we shall use two different functional forms for w_E :

$$w_E = -w_0 \sin\left(\frac{\pi y}{2b}\right) \quad (2.6a)$$

and

$$w_E = -w_0 \left(1 - \frac{|y|}{b}\right) \quad (2.6b)$$

where $y = b(-b)$ is the northern (southern) boundary of the gyre. Note that in a subtropical gyre w_E is negative so w_0 in (2.6) is positive. The introduction of two different functional forms for w_E is purely for convenience; (2.6a) and (2.6b) produce qualitatively similar flow patterns. Although the streamlines produced by (2.6b) have "kinks" at $y = 0$, where $\frac{dw_E}{dy}$ is discontinuous, it is usually easier to

visualize the flow produced by this forcing pattern. w_B in (2.6a) on the other hand has been used frequently in previous studies (e.g., Stommel, 1948; Holland, 1982). The barotropic streamfunction calculated from (2.5) will be written as

$$\psi_B = \Psi \left(1 - \frac{x}{a} \right) f_n(y) \quad (2.7)$$

where

$$\Psi = \frac{f_0 w_0 a}{\beta H} \quad (2.8a)$$

$$f_1(y) = \sin \left(\frac{\pi y}{2b} \right) \quad (2.8b)$$

$$f_2(y) = \left(1 - \frac{|y|}{b} \right). \quad (2.8c)$$

The familiar pattern in Figure 1 is the barotropic streamfunction produced by (2.6a).

The calculation of the barotropic mode is as far as classical circulation theory goes. The theory presented by RYa and b is now used to determine the vertical distribution of ψ_B . We begin by focusing on the middle layer (i.e., the lower of the two active layers).

c. The geostrophic contours in the middle layer. Since the two active layers have equal thicknesses, and the density jumps are also equal, the middle layer potential vorticity is essentially:

$$q_2 = \beta y + F(\psi_1 - 2\psi_2)$$

or from the definition of ψ_B :

$$q_2 = \beta y + \hat{F} \psi_B - 3F \psi_2 \quad (2.9)$$

$$\hat{F} = HF/H_1.$$

Since the dissipation is weak in the lower layer the general solution of (2.2b) is

$$q_2 = Q(\psi_2) \quad (2.10)$$

where Q is some as yet undetermined function of ψ_2 . A little thought shows that (2.9) and (2.10) imply that ψ_2 and q_2 are functions of the known quantity:

$$\hat{q}_2 = \beta y + \hat{F} \psi_B.$$

Thus the geostrophic contours in the lower layer (i.e., the free flow paths) are determined once and for all. The function \hat{q}_2 corresponding to (2.6a) is contoured for various values of $\Psi \hat{F} / \beta$ in Figure 2. The contours are closed in the northwest of the basin; the extent of this region increases as $\Psi \hat{F} / \beta$ increases. If the forcing is weak then all of the geostrophic may be blocked. For instance using (2.6b) it is easy to show that closed \hat{q}_2 contours exist only if:

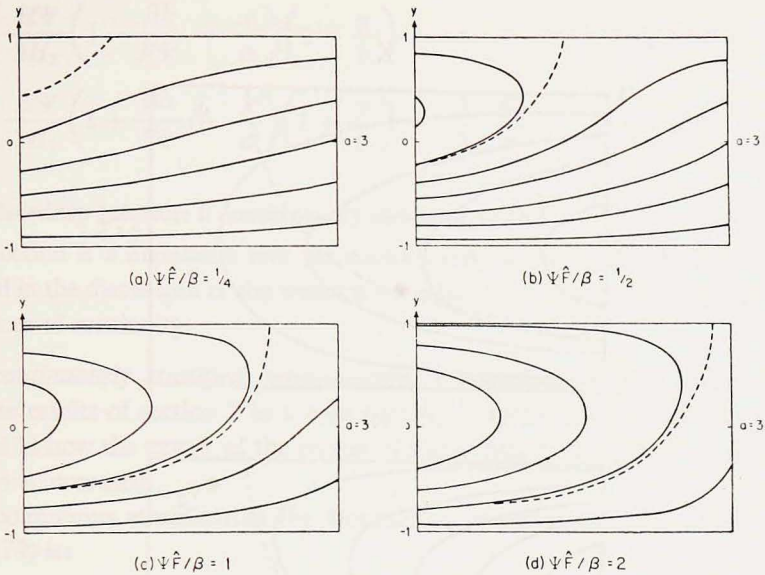


Figure 2. The function $\hat{q} = y + (\Psi\hat{F}/\beta) (a - x)\cos\left(\frac{\pi}{2} \frac{y}{b}\right)$ for various values of $\Psi F/\beta$. The outermost closed contour is dashed. As the strength of the forcing increases the closed contour region expands southward and eastward.

$$\gamma \equiv \frac{\hat{F}\Psi}{\beta b} > 1 .$$

In the regions threaded by blocked geostrophic contours we must have $\psi_2 \cong 0$ since there can be no flow through the eastern boundary. In the shielded region of closed contours there can be substantial lower layer flows which pass through the western boundary layer. As emphasized in RYb, in the absence of dissipation one is free to choose an arbitrary functional relationship between q_2 and \hat{q}_2 . Hence we have an infinite number of possible solutions. This difficulty is overcome using the generalized Batchelor-Prandtl theorem given by RYa which shows that if the dominant dissipative process is lateral diffusion of q_2 , then the potential vorticity is homogeneous in the closed region.

d. Determination of ψ_2 in the closed region. As in RYa,b we argue that substantial lower layer flows are confined to the region where the \hat{q}_2 contours close and the streamfunction in this region is determined by requiring that the potential vorticity be uniform. Thus from (2.9):

$$\psi_2 = \frac{1}{3F} [\hat{q}_2 - q_2] \quad \text{inside closed } q_2 \text{ contours} \quad (2.11a)$$

$$\psi_2 = 0 \quad \text{elsewhere} . \quad (2.11b)$$

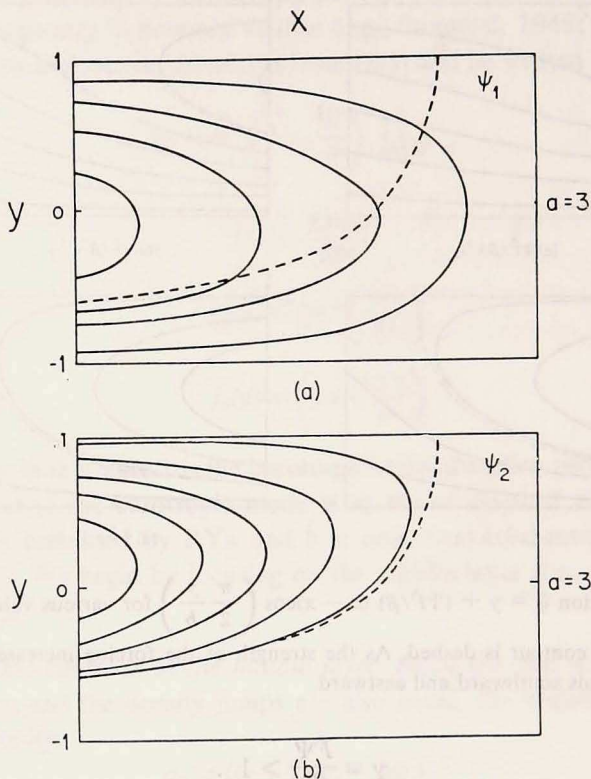


Figure 3. The streamline pattern corresponding to (2.11). The dashed curve is the outermost closed \hat{q}_2 contour inside of which the potential vorticity is uniform in the lower layer. Outside this region, $\psi_2 = 0$.

The constant value of q_2 in (2.11a) is chosen to make ψ_2 continuous on the outermost closed \hat{q}_2 contour. Since ψ_B is zero on $y = b$ it follows that $\hat{q}_2 = \beta b$ is the outermost closed q_2 contour. Thus $q_2 = \beta b$ is constant value of q_2 in the region of closed \hat{q}_2 contours.

Now that ψ_2 is known, (2.11), ψ_1 is calculated from (2.4). The streamline pattern calculated from (2.11), (2.4) and (2.6b) is sketched in Figure 3 for the special case $\hat{F}\Psi/\beta = 1$, $a = 3$, $b = 1$. This figure summarizes the results of this section; note the north-south asymmetry of the flow and the poleward shift of the gyre center with depth. These realistic features will reappear in the continuously stratified model of section 3.

For future reference we record the explicit expressions for ψ_2 when ψ_B is given by (2.7) and (2.8c):

$$\psi_2 = \begin{cases} \frac{H\Psi}{3H_1} \left(1 - \frac{\beta b}{\hat{F}\Psi} - \frac{x}{a} \right) \left(1 - \frac{y}{b} \right) & \text{if } y > 0 \\ \frac{H\Psi}{3H_1} \left(1 + \frac{\beta b}{\hat{F}\Psi} - \frac{x}{a} \right) \left(1 + \frac{y}{b} \right) - \frac{2}{3} \frac{\beta b}{F} & \text{if } y < 0 \end{cases} \quad (2.12a)$$

$$\psi_2 = \begin{cases} \frac{H\Psi}{3H_1} \left(1 - \frac{\beta b}{\hat{F}\Psi} - \frac{x}{a} \right) \left(1 - \frac{y}{b} \right) & \text{if } y > 0 \\ \frac{H\Psi}{3H_1} \left(1 + \frac{\beta b}{\hat{F}\Psi} - \frac{x}{a} \right) \left(1 + \frac{y}{b} \right) - \frac{2}{3} \frac{\beta b}{F} & \text{if } y < 0 \end{cases} \quad (2.12b)$$

3. The Sverdrup interior: a continuously stratified model

This section is a digression into the continuously stratified theory. Readers more interested in the discussion of the western boundary layer can go directly to section 4 without loss of continuity.

a. The continuously stratified quasigeostrophic equations. In this section we will extend the results of section 2 to a continuously stratified model. We are especially interested in how the extent of the region of subsurface flow changes as the vertical resolution is increased.

With continuous stratification the Boussinesq potential vorticity equation (Pedlosky, 1979) is:

$$J(\psi, q) = (\text{dissipation}) \quad (3.1a)$$

$$q = \psi_{xx} + \psi_{yy} + \left(\frac{f_0^2}{N^2} \psi \right)_z + \beta y \quad (3.1b)$$

where ψ is the streamfunction and q is the potential vorticity. The vertical velocity is given by

$$w = -f_0 N^{-2} J(\psi, \psi_z) \quad (3.2)$$

so that the boundary condition at the base of the mixed layer, $z = 0$, is

$$w_E = -f_0 N^{-2} J(\psi, \psi_z) |_{z=0} \quad (3.3)$$

The total density field is

$$\rho = \rho_0 \left\{ 1 - g^{-1} \int^z N^2 dz' - f_0 g^{-1} \psi_z \right\} \quad (3.4)$$

where g is gravitational acceleration, ρ_0 is the average density, N the buoyancy frequency and ψ_z the perturbation due to the wind-driven flow.

We now nondimensionalize (3.1)-(3.4) using the following scalings (\bullet denotes a nondimensional quantity):

$$(x, y) = b(x_\bullet, y_\bullet) \quad (3.4a)$$

$$\psi = Ub \psi_\bullet \quad (3.4b)$$

$$q = \beta b q_\bullet \quad (3.4c)$$

$$z = lz_\bullet \quad (3.4d)$$

$$w = Ww_\bullet \quad (3.4e)$$

where W is a measure of the amplitude of the externally imposed w_B and, as in section 2, b is a north-south length scale. l is the vertical length scale of the wind-driven flow and U is horizontal velocity scale of the flow. The internal variables l and U are expressed in terms of external variables using two physical arguments:

- (i) the planetary scale vorticity balances applies: $\beta v = fw_z$ so $\beta Ul \sim fW$
- (ii) vortex stretching balances the β effect so that the geostrophic contours close:

$$\beta y \sim \left(\frac{f_0}{N}\right)^2 \psi_{zz} \text{ so } \beta bl^2 \sim \left(\frac{f_0}{N_0}\right)^2 Ub \text{ where } N_0 \text{ is a typical value of the}$$

buoyancy frequency in the wind-driven part of the water column.

Solving the scaling relations above gives:

$$U = (N_0 W)^{2/3} \beta^{-1/3} \quad (3.5a)$$

$$l = f_0 (N_0 \beta)^{-2/3} W^{1/3}. \quad (3.5b)$$

The nondimensional potential vorticity is (dropping the \cdot 's):

$$q \cdot = \epsilon^2 (\psi_{xx} + \psi_{yy}) + (F \psi_z)_z + y \quad (3.6)$$

where

$$F = N_0^2 / N^2 \quad (3.7a)$$

$$\epsilon^2 = U \beta / b^2. \quad (3.7b)$$

As in section 2 $\epsilon^2 \ll 1$ so the relative vorticity is negligible in the Sverdrup interior. The density field in terms of nondimensional variables is

$$\rho = \rho_0 \left[1 - N_0^2 g^{-1} \left\{ \int^z F^{-1} dz' + \left(\frac{\beta b}{f_0}\right) \psi_z \right\} \right]. \quad (3.8)$$

This last relation shows that the quasigeostrophic approximation is valid to the extent that $\left(\frac{\beta b}{f_0}\right)$ is small.

b. The depth of the wind-driven gyre. Now suppose that the wind-driven circulation lies between $z = 0$ and $z = -D(x, y)$; the surface $z = -D(x, y)$ is a "bowl" which vertically bounds the wind-driven flow. Outside the region $z > -D$ the fluid is motionless. Thus $z = -D$ is a "level of no motion." The goal of this section is to calculate D in terms of the forcing $w_B(x, y)$ and the basin geometry. We will assume that the buoyancy frequency is constant; this assumption is not essential. Because of (3.7a) we can take $F = 1$.

In accord with the assumption that the dissipation in (3.1a) is weak:

$$q = Q(\psi, z) \quad (\text{if } 0 > z > -D)$$

and then using the homogenization arguments given by RYa and b:

$$\frac{\partial Q}{\partial \psi} = 0 \quad (\text{if } 0 > z > -D(x, y))$$

so that:

$$q = y + \psi_{zz} = y_0(z) \quad (\text{if } 0 > z > -D(x,y)) \quad (3.9)$$

where $y_0(z)$ is the value of the potential vorticity at level z .

Outside the bowl $0 > z > -D(x,y)$ the wind-driven flow vanishes so that in the absence of deep thermohaline forcing or flow imposed by distant sources of fluid (e.g., deep water formation):

$$\psi = 0 \quad (\text{if } z < -D(x,y)) . \quad (3.10)$$

Now as in section 2 (see the discussion after (2.11)) the function $y_0(z)$ in (3.9) is determined from the matching condition at the outermost closed geostrophic contour. Anticipating that these contours will resemble those of the layered model shown in Figure 2, we see that they are contiguous with the northern boundary of the gyre where $q = y = 1$ in our nondimensional units. This suggests that

$$y_0(z) = 1 . \quad (3.11)$$

Since the comparison with the layered model in section 2 may not be entirely convincing we will assume that y_0 is a constant (rather than a function of z) and examine the consequences of the alternatives to (3.11). We hope this will further motivate the choice $y_0 = 1$.

c. *Solution of (3.9).* The solution of (3.9) which satisfies:

$$\psi = \psi_z = 0 \quad \text{on } z = -D(x,y)$$

is:

$$\psi = \frac{1}{2} (z + D)^2 (y_0 - y) \quad \text{if } -D < z < 0 \quad (3.12a)$$

$$\psi = 0 \quad \text{if } z < -D . \quad (3.12b)$$

$D(x,y)$ is determined by requiring that (3.12a) satisfy the upper boundary condition (3.3). The vertical velocity from (3.2) is

$$w = \frac{1}{2} (z + D)^2 (y_0 - y) \left(\frac{\partial D}{\partial x} \right) \quad (3.13)$$

so that (3.12b) implies

$$\frac{\partial}{\partial x} (D^3) = 6(y_0 - y)^{-1} w_B$$

or

$$D^3 = 6(y_0 - y)^{-1} \psi_B \quad (3.14)$$

where

$$\psi_B = (x - a) w_B \quad (3.15a)$$

= barotropic streamfunction

$$a = \text{position of eastern boundary} . \quad (3.15b)$$

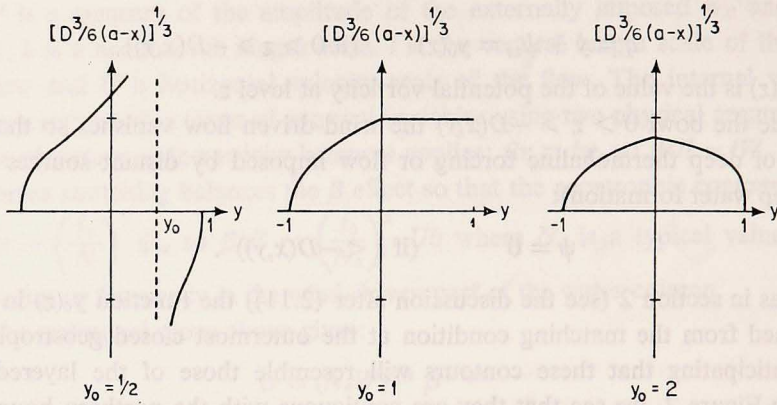


Figure 4. The shape of the bowl bounding the wind-driven circulation. This figure illustrates the consequences of varying the constant y_0 . In the text it is argued that $y_0 = 1$ is the correct choice.

d. *A model of the Ekman pumping:* $w_B = -[1 - |y|]$. The streamline pattern corresponding to (3.12) and (3.14) is surprisingly difficult to visualize. It is helpful to consider the simple forcing function

$$w_B = -[1 - |y|] \quad (3.16)$$

since in this case the streamlines are simple algebraic curves. This is only for convenience, all plausible models of the Ekman pumping in a subtropical gyre, such as (2.6a), produce qualitatively similar patterns.

With w_B given by (3.16), $D[6(a-x)]^{-1/3}$ is plotted against y in Figure 4. Clearly the choice $y_0 < 1$ leads to unphysical results and can be excluded. The choice $y_0 > 1$ leads to superficially reasonable results. There are analogous patterns in the 2 1/2 layer model of section 2; they correspond to picking one of the inner closed contours in Figure 2b to bound the circulation in the middle layer. Such a configuration cannot persist since the upper layer flow exerts a stress around the available closed contours at the rim of the bowl and eventually accelerates a flow around them. This process deepens the bowl until all the closed contours have a mean flow around them. The limiting situation, in which the bowl is as large as possible and abuts the northern boundary, corresponds to $y_0 = 1$. Although the above discussion has been couched in terms of the layer model, similar considerations must apply in a continuously stratified model; note how the bowl deepens and moves up against the northern boundary as y_0 decreases to 1 in Figure 4.

To summarize, the streamfunction is

$$\psi = \begin{cases} \frac{1}{2}(z+D)^2(1-y) & -D < z < 0 \\ 0 & z < -D \end{cases} \quad (3.17a)$$

$$(3.17b)$$

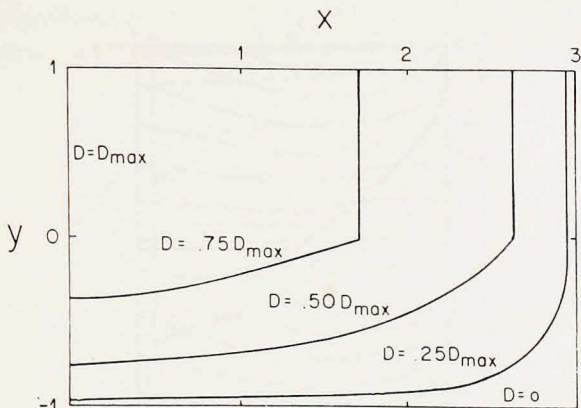


Figure 5. The depth of the wind-driven circulation as a function of position from (3.14) and (3.16). The bowl is deepest at the line segment $x = 0, 0 < y < 1$. The circulation becomes shallower as one moves south and east.

where

$$D = [6(1 - y)^{-1} (x - a) w_E(y)]^{1/3}. \tag{3.18}$$

The surface $z = -D(x,y)$ bounds the region containing the wind-driven circulation from which the potential vorticity gradients have been expelled. The region is deepest in the northwest corner of the basin and shoals as one moves south and east, see Figure 5. The streamlines corresponding to (3.17) are sketched in Figure 6. This sequence clearly shows how the wind-driven flow is compressed into the northwest corner of the basin as one moves downward. In Figure 7 we show meridional density sections through the gyre at $x = 0, x = \frac{1}{3} a$ and $x = \frac{2}{3} a$. At the eastern boundary, $x = a, D = 0$ and the isopycnals are undisturbed. Note how the spacing between isopycnals increases as one moves poleward; as explained in RYb this en-

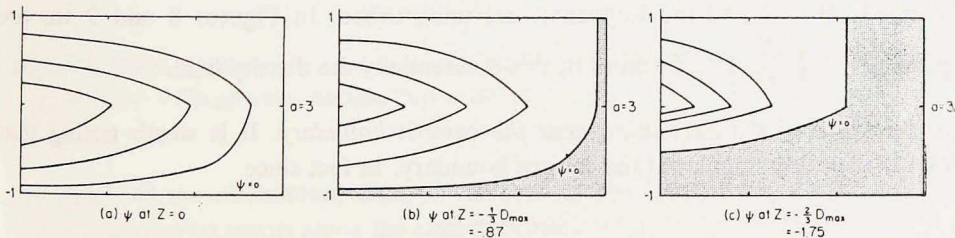


Figure 6. The streamlines from (3.17a) at various depths in the wind-driven gyre. This is no motion in the stippled regions outside the surface $z + D = 0$. The flow is confined to the region of uniform potential vorticity.

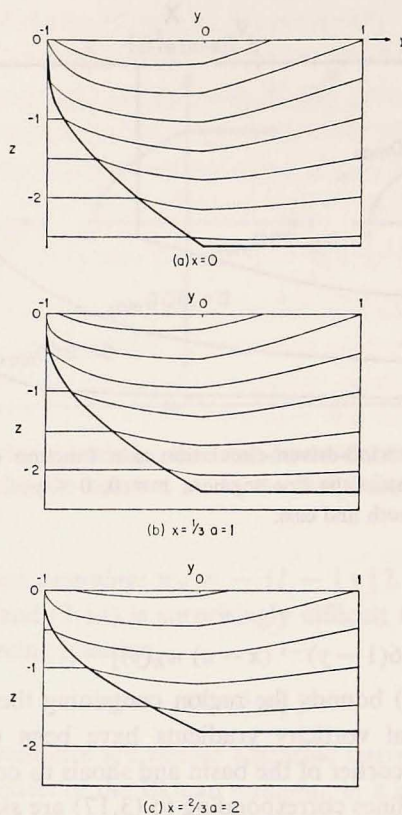


Figure 7. Three meridional density sections showing $z + \frac{1}{3} \psi_z$ with $w_B = -[1 - |y|]$. The heavy curve is $z = -D$ while the light curves are isopycnals. Note how the isopycnal spacing increases as one moves poleward so that the potential vorticity is uniform.

sures that the potential vorticity is uniform within the gyre. In Figure 8 zonal density sections through the gyre at $y = \frac{2}{3}$, $y = 0$, and $y = -\frac{2}{3}$ are shown. At $y = -1$, $D = 0$ and the isopycnals are undisturbed. In Figures 8 and 9 we are plotting $z + \left(\frac{\beta b}{f_0}\right) \psi_z$. From (3.8) this is essentially the density field.

e. Structure of the circulation near the eastern boundary. It is worth noting that (3.12) is weakly singular at the eastern boundary. In fact since

$$v = \psi_x \\ \propto (x - a)^{-2/3}$$

the north-south velocity becomes infinite as $x \rightarrow a$. This singularity occurs because

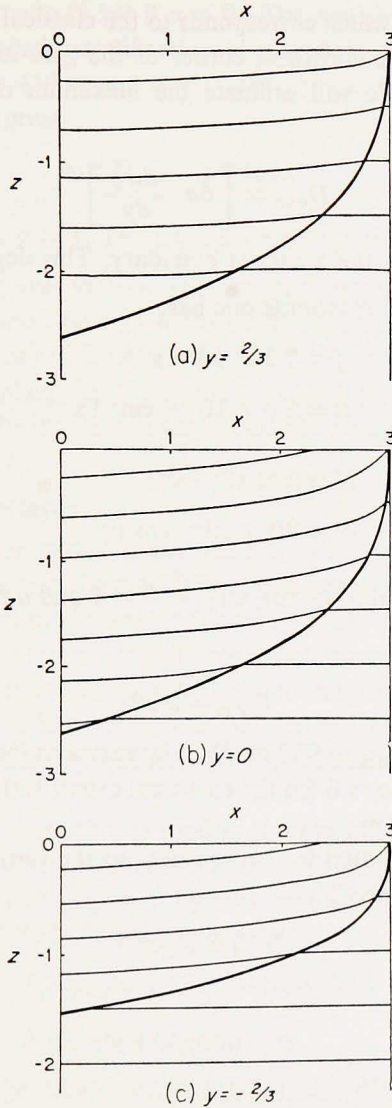


Figure 8. Three zonal density sections showing $z + \frac{1}{3} \psi_z$ with $w_B = -[1 - |y|]$. The heavy curve is $z = -D(x,y)$ while the light curves are isopycnals.

the depth of the circulation, $D(x,y)$, vanishes at the eastern boundary. Thus all of the Sverdrup transport along the eastern boundary is compressed into a “jet.”

f. How deep is the “level of no motion”? This section would be incomplete without some numerical estimates of the depth of the gyre. It is apparent from Figure 5 that

the surface $z = -D(x,y)$ (which corresponds to the classical notion of a "level of no motion") is deepest in the northwest corner of the gyre and shoals as one moves to the south and east. We will estimate the maximum depth of the circulation. From (3.18):

$$D_{\max} = \left[6a \frac{dw_E}{dy} \right]^{1/3} \quad (3.19)$$

where $\frac{dw_E}{dy}$ is evaluated at the northern boundary. This depth is measured in units of l defined in (3.5b). At 30° latitude one has:

$$f = 7.3 \times 10^{-5} \text{ s}^{-1}$$

$$\beta = 2.0 \times 10^{-13} \text{ cm}^{-1} \text{ s}^{-1}$$

and typically:

$$N \cong 5 \times 10^{-3} \text{ s}^{-1}$$

$$W \cong 20 \times 10^{-5} \text{ cm s}^{-1}$$

so that $l \cong 430$ m. Now from (3.19), with $\frac{dw_E}{dy} = 1$ and $a = 2$ (i.e., a square basin) it follows that

$$D_{\max} = 2.29$$

or in dimensional units $D_{\max} \cong 980$ m. D_{\max} increases as the aspect ratio of the gyre increases. For instance if $a = 6$ (so the east-west extent is three times the north-west extent) then $D_{\max} = 1400$ m.

The depth of the circulation is also sensitive to the form assumed for the buoyancy frequency. For instance if

$$N(z) = N_0 e^{-bz} \quad (3.20)$$

in dimensional units then

$$q = (e^{\alpha z} \psi_z)_z + y \quad (3.21a)$$

$$\alpha = 2bl \quad (3.21b)$$

in the nondimensional units defined in (3.4) and (3.5). The preceding calculation can be repeated and one finds

$$\psi = (1-y)[e^{\alpha z} \{\alpha^{-1}(D+z) - \alpha^{-2}\} + e^{-\alpha D} \alpha^{-2}] \quad (3.22)$$

where $D(x,y)$ is obtained by solving the transcendental equation:

$$[(a-x)w_E(y)/(1-y)] = \frac{1}{3} D^3 [1 + e^{-\gamma} 6\gamma^{-2}(1+2\gamma^{-1}) + \{6\gamma^{-2}(1-2\gamma^{-1}) - 1\}] \quad (3.23a)$$

$$\gamma = \alpha D \quad (3.23b)$$

(Note how (3.23a) reduces to (3.14) if $\alpha \rightarrow 0$.) The most important qualitative effect of the slightly more realistic stratification in (3.20) is to deepen the circulation. Suppose for instance $l \cong 430$ m and $b = (1300 \text{ m})^{-1}$ so that $\alpha \cong .66$. Numerically solving (3.23a) for D_{\max} gives

$$D_{\max} = 1,340 \text{ m}$$

if $a = 2$ and $\frac{dw_E}{dy} = 1$ at $y = 1$. The previous estimate of D_{\max} (which corresponds to $\alpha = \gamma = 0$ in (3.23a)) was 980 m. This tendency for the gyre to deepen is even more noticeable if the aspect ratio is increased. For instance if $a = 6$ one finds that $D_{\max} \cong 2,300$ m (recall that with $\alpha = 0$ and $a = 6$ we had $D_{\max} \cong 1,400$ m). These remarks may help to explain the apparently greater depth of the subtropical gyres in the North and South Pacific, as compared with the Atlantic.

4. The western boundary layer

The interior circulation patterns discussed in the previous two sections, and shown in Figures 3 and 6, must be closed by appending western boundary layers.

The calculation here is motivated by Moore's (1963) boundary layer model. In the southern part of the basin we will construct inertial boundary layers (e.g., Charney, 1955). In the northern part there is a damped stationary Rossby wave which provides the dissipation required to balance the forcing in the upper layer. The lower layer has uniform potential vorticity throughout, even in the damped stationary Rossby wave.

In homogeneous circulation theory (and in the top layer of the two layer model considered here) the fluid loses potential vorticity in the Sverdrup interior due to Ekman pumping and so must regain it by frictional flux. The frictional mechanism we adopt here is lateral diffusion of potential vorticity:

$$J(\psi_1, q_1) = \kappa \nabla^2 q_1 + (f_0 w_E / H_1) \quad (4.1a)$$

$$J(\psi_2, q_2) = \kappa \nabla^2 q_2. \quad (4.1b)$$

This is consistent with the philosophy of RYa,b and Rhines and Holland (1979) where it was argued that the dominant effect of mesoscale eddies on the mean flow is lateral diffusion of potential vorticity. In an inertial boundary layer the right-hand side of (4.1) is negligible and there is a functional relationship between ψ_n and q_n .

The analysis in this section is done using w_E in (2.6b) and ψ_B in (2.7) and (2.8c):

$$\begin{aligned} H\psi_B &= H_1(\psi_1 + \psi_2) \\ &= H\Psi \left(1 - \frac{x}{a} \right) \left(1 - \frac{|y|}{b} \right). \end{aligned}$$

This particular choice is convenient because it allows one to obtain explicit solu-

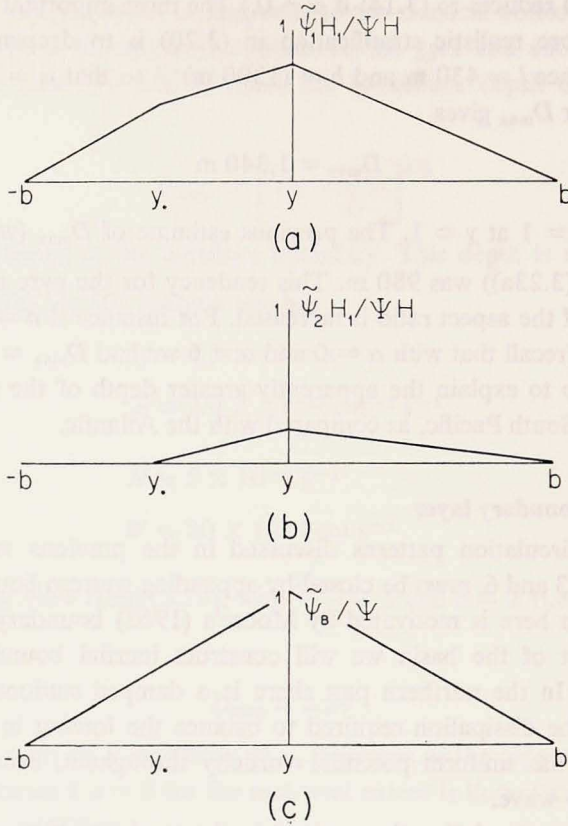


Figure 9. The outer streamfunctions $\tilde{\psi}_1$, $\tilde{\psi}_2$ and $\tilde{\psi}_B$ as functions of y at $x = 0$. The Ekman pumping is given by (2.6b) and $\beta b/F\Psi = 1/3$.

tions. It is expected that other forcing patterns such as (2.6a) lead to qualitatively similar flow fields.

a. *Formation of the boundary layer problem.* We use the “equivalent two layer” equations of section 2. The interior solutions found in that section will be denoted by \sim in this section, thus

$$\psi_n = \tilde{\psi}_n + \phi_n \tag{4.2}$$

[total streamfunction] = [interior solution] + [boundary layer correction]

In Figure 9 we plot $\tilde{\psi}_1$ and $\tilde{\psi}_2$ as functions of y at the western boundary layer. y_* denotes the position at which the curve $\tilde{\psi}_2 = 0$ cuts $x = 0$ if it is extrapolated through the boundary layer. The value $\psi_1(0, y_*)$ will be denoted by ψ_{1*} . Since the Ekman pumping is given by (2.6b) the streamfunctions are simply straight line segments. It is easy to see that

$$y_*/b = (1 - \gamma)/(1 + \gamma) \quad (4.3a)$$

$$\psi_{1*} = (H\Psi/H_1) (2\gamma)/(1 + \gamma) \quad (4.3b)$$

where

$$\gamma = \hat{F}\Psi/\beta b \quad (4.3c)$$

is a measure of the strength of the forcing. For the geostrophic contours to close γ must be greater than 1. Note how $y_* \rightarrow -b$ as the strength of the forcing increases. This corresponds to the region of uniform q_2 expanding and filling the whole basin.

Figure 9 shows that the western boundary divides naturally into three regions.

Before becoming involved in a rather tedious analysis we will state our conclusions. As one might have expected from intuition based on homogeneous theory, inertial boundary layers are possible in the southern half of the basin where \bar{u}_1 and \bar{u}_2 are negative. The length scale of these layers is $F^{-1/2}$ (or equivalently $(u_1/\beta)^{1/2}$). In the northern half of the basin, where the fluid leaves the boundary layer, inertial boundary layers are not possible. Instead there is a slowly decaying, stationary baroclinic Rossby wave. Because the lower layer potential vorticity is uniform this wave is neutrally stable with respect to baroclinic instability.

b. Region I: $-b < y < y_*$. In region I $\bar{\psi}_2 = 0$ and $\bar{u}_1 < 0$ so that one expects that the upper layer can form an inertial boundary layer while the lower layer remains at rest.

It is easy to eliminate y between the outer solutions $\bar{\psi}_1(0,y)$ and $q_1(0,y)$ and so obtain the functional relationship between ψ_1 and q_1 :

$$q_1 = -F \frac{\gamma - 1}{\gamma} \psi_1 - \beta b \quad \text{if } 0 < \psi_1 < \psi_{1*} \quad (4.4)$$

Naturally the above only applies if $0 < \psi_1 < \psi_{1*}$ since only these streamlines impinge on the western boundary in region I. Since the boundary layer is inertial the functional relationship (4.4) is preserved inside the boundary layer and can be used to calculate ψ_1 :

$$\psi_1 = \bar{\psi}_1 \{1 - e^{-\alpha \sqrt{Fx}}\} \quad (4.5)$$

where α^{-1} is the decay of the boundary layer in region I where q_1 and ψ_1 are related by (4.4) and $\psi_2 = 0$. In terms of the other parameters

$$\alpha^2 = \beta b H_1 / \Psi H F \quad (4.6a)$$

$$= \gamma^{-1} \quad (4.6b)$$

c. Region II: $y_* < y < 0$. In this region \bar{u}_1 and \bar{u}_2 are both negative and so once again inertial boundary layers are possible. If $\bar{\psi}_{1*} > \psi > 0$ then (4.4) is still the functional relationship between q_1 and ψ_1 since these streamlines lead back to region I. If $\psi_1 > \psi_{1*}$ however the streamlines originate in the interior adjacent to

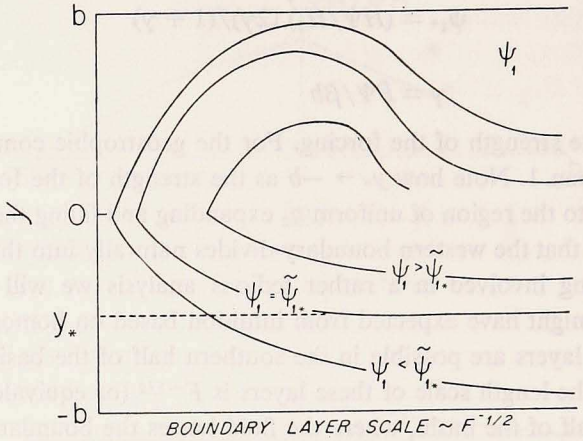


Figure 10. A schematic illustration of the boundary layer solution. When $y < 0$ the boundary layers are inertial. To the left of $\psi_1 = \bar{\psi}_1$, the functional relationship between ψ_1 and q_1 is given by (4.4). To the right of $\psi_1 = \bar{\psi}_1$, it is given by (4.7). When $y > 0$ the flow returns to the interior via a stationary baroclinic Rossby wave.

region II and the functional relationship is calculated by eliminating y between $\bar{q}_1(0,y)$ and $\bar{\psi}_1(0,y)$, see Figure 10. One finds

$$q_1 = A(\gamma) F \psi_1 + B(\gamma) \beta b \quad (4.7)$$

where A and B are uninformative functions of γ :

$$A(\gamma) = \frac{-\gamma + 5}{2\gamma + 1} \quad \text{and} \quad B(\gamma) = \frac{-1 + 2\gamma - 6\gamma^3}{2\gamma - 1}.$$

The functional relationship between q_2 and ψ_2 is trivial: the lower layer streamlines which lead into region II originate in the region of uniform potential vorticity so q_2 is constant in region II and equal to its value in the Sverdrup interior:

$$q_2 = \beta b. \quad (4.8)$$

Now the solution of the boundary layer equations in region II is straightforward but tedious because the functional relationship between q_1 and ψ_1 changes at the streamline $\bar{\psi}_1$. Rather than reproduce all the details we will show the boundary layer equations have solutions with the correct asymptotic behavior as $x \rightarrow \infty$. In the transition region between the boundary layer and the Sverdrup interior the relation between q_1 and ψ_1 is (4.7) and the boundary layer equations are

$$\psi_{1xx} - F(1 + A)\psi_1 + F\psi_2 = -\beta y - B\beta b \quad (4.9a)$$

$$\psi_{2zz} + F\psi_1 - 2F\psi_2 = -\beta y + \beta b. \quad (4.9b)$$

A particular solution of the above equations is just the outer solution $(\bar{\psi}_1, \bar{\psi}_2)$. The boundary layer corrections in (4.2) then satisfy the homogeneous equations

$$\phi_{1xx} - F(1 + A)\phi_1 + F\phi_2 = 0 \quad (4.10a)$$

$$\phi_{2xx} + F\phi_1 - 2F\phi_2 = 0 \quad (4.10b)$$

which can be solved by finding the normal modes:

$$\begin{Bmatrix} \phi_1 \\ \phi_2 \end{Bmatrix} = \begin{Bmatrix} \hat{\phi}_1 \\ \hat{\phi}_2 \end{Bmatrix} e^{-\sqrt{F\alpha x}}.$$

One finds that α is a solution of

$$\alpha^4 - (3 + A)\alpha^2 + (1 + 2A) = 0. \quad (4.11)$$

If (4.11) has two positive roots then (4.10) has two decaying solutions and it is clear we can construct solutions which satisfy the matching conditions at $x = \infty$. It is easy to see that this is the case if $A > -\frac{1}{2}$. The explicit expression for A shows that A is greater than $-\frac{1}{2}$ if $\gamma > 1$. This latter condition is necessary and sufficient for the existence of region II in the first place.

To summarize: in regions I and II one can construct an inertial boundary layer. This is to be expected since the interior velocities are directed toward the coast in these regions. The solutions so constructed do not satisfy the no slip condition (as they should because of the $\kappa \nabla^4 \psi_n$ on the right-hand side of (4.1)). Provided κ is sufficiently small this can be remedied by inserting thin viscous sublayers within the inertial boundary layer (see Pedlosky, 1979, section 5.9).

We turn now to region III where the fluid in both layers leaves the boundary layers. In this region it is not possible to construct an inertial boundary layer.

d. Region III: $0 < y < b$. It is clearly impossible for the boundary layer in region III to be inertial since the functional relationship between $\bar{q}_1(0, y)$ and $\bar{\psi}_1(0, y)$ is:

$$\bar{q}_1 = \beta b - C(\gamma)F\psi_1 \quad (4.12a)$$

$$C(\gamma) = \frac{\gamma + 5}{2\gamma + 1} \quad (4.12b)$$

and this is inconsistent with both (4.4) and (4.7).

Instead we shall follow Moore (1963) and analyze (4.1) in the transition region between the boundary layer proper and the interior flow. In this region

$$\bar{\psi}_1 \gg \phi_1 \quad (4.13)$$

and so the nonlinear terms in (4.1) are insignificant and we have

$$\bar{u}_1[\phi_{1xx} + F(\phi_2 - \phi_1)]_x + \phi_{1x}\bar{q}_{1y} = [\phi_{1xx} + F(\phi_2 - \phi_1)]_{xx}. \quad (4.14)$$

The above equation can be integrated once. The constant of integration is zero since $\phi_n \rightarrow 0$ as $x \rightarrow \infty$:

$$[\phi_{1xx} + F(\phi_2 - \phi_1)] + C(\gamma)F\phi_1 = \bar{u}_1^{-1}\kappa[\phi_{1xx} + F(\phi_2 - \phi_1)]_x \quad (4.15)$$

where (4.12a) was used to eliminate \bar{q}_{1y}/\bar{u}_1 . Now guided by the fact that the potential vorticity in the lower layer is uniform we have

$$\phi_{2xx} + F(\phi_1 - 2\phi_2) = 0 \quad (4.16)$$

We now solve (4.15) and (4.16) by looking for a solution in the form:

$$(\phi_1, \phi_2) = (\phi_1, \phi_2)e^{-\alpha\sqrt{Fx}}.$$

One finds that α satisfies the fifth order polynomial:

$$\alpha^4 + [C - 3]\alpha^2 + [1 - 2C] = - \left(\frac{\kappa F^{1/2}}{\bar{u}_1} \right) [\alpha^5 - 3\alpha^3 + \alpha] \quad (4.17)$$

For small values of $\left(\frac{\kappa F^{1/2}}{\bar{u}} \right)$ solutions can be found in a perturbation expansion

$$\alpha = \alpha_0 + \left(\frac{\kappa F^{1/2}}{\bar{u}_1} \right) \alpha_1 + \dots$$

The first order problem is a quadratic in α_0^2 . There are two real roots, one is positive, the other negative. The positive root corresponds to an exponentially decaying normal mode; α_1 is an unimportant correction to the decay scale. The negative root corresponds to a mode which has an oscillatory x -structure; i.e., a standing Rossby wave. The small correction, $\left(\frac{\kappa F^{1/2}}{\bar{u}_1} \right) \alpha_1$, is real:

$$\alpha_1 = - \frac{\alpha_0^4 - 3\alpha_0^2 + 1}{4\alpha_0^2 + 2(C - 3)}$$

and ensures that the wave decays slowly on a scale $\bar{u}/\kappa F$. Since the wavelength of the wave is $F^{-1/2}$ there are roughly $\bar{u}/\kappa F^{3/2}$ oscillations before decay.

Finally it's worth remarking that each of the solutions obtained from (4.17) is, by itself, an exact solution of the nonlinear boundary layer equations. That is the nonlinear terms, which were neglected to obtain (4.14), happen to vanish identically. Of course because the equations are nonlinear these solutions cannot be superimposed to form more general solutions or satisfy boundary conditions.

5. Some speculations

It is interesting that the stationary baroclinic Rossby wave described in the previous section is, according to Charney-Stern criterion, neutrally stable with respect to baroclinic instability. This is of course because the potential vorticity gradient vanishes in the lower layer.

This leads us to speculate about the way in which the final statistically steady circulation is established in numerical models such as those of Holland (1982) and McWilliams and Chow (1981). (We might optimistically hope these speculations apply even to the ocean.)

Imagine a set of numerical experiments in which the strength of the forcing ranges from very weak to quite strong. When the forcing is weak all of the wind-driven flow is in the top, directly forced layer. Moreover, this configuration is baroclinically stable since the potential vorticity field is dominated by β everywhere. As the strength of the forcing is increased the geostrophic contours in the lower layer are increasingly distorted (e.g., Fig. 2). Eventually closed lower layer geostrophic contours appear. Since this necessitates a reversal of the potential vorticity gradient, the appearance of closed lower layer geostrophic contours also heralds the onset of baroclinic instability. The baroclinically unstable region is in the northwest where fluid is leaving the western boundary layer and entering the interior. It is plausible that disturbances amplify in this region and eventually equilibrate by inducing a mean flow in the lower layer which removes the reversal in sign of the mean potential vorticity gradient (for more details of this process within the context of weakly nonlinear instability theory see Pedlosky, 1970, 1971 and 1972). To accomplish this equilibration a large fraction of the total transport must migrate down to the lower layer.

Now, if the equilibration described above is to occur as economically as possible, the mean potential vorticity gradient will be reduced to zero. This argument suggests that baroclinic instability, localized in the northwest, produces a source region of uniform potential vorticity. The flow through this source region fills up all of the closed lower layer geostrophic contours with fluid which has uniform potential vorticity. This scenario is consistent with the assumptions of RY_{a,b}. The boundary layer analysis of section 4 has, however, suggested a more detailed picture than the quasigeostrophic Prandtl-Batchelor theorem; we are led to expect that the down gradient potential vorticity flux is localized in the northwest where strong baroclinic instability occurs.

There is more to be said about western boundary current dynamics in this family of circulation models. A linear-frictional closure analogous to the Stommel one-layer model has been developed in collaboration with Dr. G. Ierley of M.I.T. It involves some intricate balances where the geostrophic contours are drawn into the boundary layer. The interior solution is sensitive to western boundary dynamics, in contrast to the purely westward propagation of influence in the one-layer model.

These models encourage us to re-examine the mixing processes at work in actual boundary currents. Water-mass alteration between Cape Hatteras and the Grand Banks of Newfoundland, for example, would imply potential vorticity mixing, and should have its impact on the entire wind-gyre.

Acknowledgments. Funding was provided by the National Science Foundation grant OCE-80-23763, and by fellowships from the J. S. Guggenheim Foundation, Christs College, Cambridge, and the W.H.O.I. Summer Program in Geophysical Fluid Dynamics. This is contribution number 5131 of the Woods Hole Oceanographic Institution.

REFERENCES

- Bleck, R. and D. B. Boudra. 1981. Initial testing of a numerical ocean circulation model using a hybrid (quasi-isopycnic) vertical coordinate. *J. Phys. Oceanogr.*, *11*, 755-770.
- Charney, J. G. 1955. The Gulf Stream as an inertial boundary layer. *Proc. Nat. Acad. Sci., U.S.A.*, *41*, 731-740.
- Coats, D. A. 1981. An estimate of absolute geostrophic velocity from the density field in the northeast Pacific Ocean. *J. Geophys. Res.*, *86*, 8031-8036.
- Holland, W. R. 1982. Regions of uniform potential vorticity in an ocean circulation model with mesoscale resolution, (in preparation).
- McDowell, S., P. B. Rhines and T. Keffer. 1982. Maps of north Atlantic potential vorticity, and its relation to the general circulation. *J. Phys. Oceanogr.*, (in press).
- McWilliams, J. C. and J. H. S. Chow. 1981. Equilibrium geostrophic turbulence I: A reference solution in a β -plane channel. *J. Phys. Oceanogr.*, *11*, 921-949.
- Moore, D. W. 1963. Rossby waves in ocean circulation. *Deep-Sea Res.*, *10*, 735-748.
- Munk, W. H. 1950. On the wind-driven ocean circulation. *J. Meteorol.*, *7*, 79-93.
- Pedlosky, J. 1970. Finite amplitude baroclinic waves. *J. Atmos. Sci.*, *27*, 15-30.
- 1971. Finite amplitude baroclinic waves with small dissipation. *J. Atmos. Sci.*, *28*, 587-597.
- 1972. Limit cycles and unstable baroclinic waves. *J. Atmos. Sci.*, *29*, 53-63.
- 1979. *Geophysical Fluid Dynamics*. Springer Verlag, 624 pp.
- Rhines, P. B. and W. R. Holland. 1979. A theoretical discussion of eddy driven mean flows. *Dyn. Atmos. and Oceans*, *3*, 289-325.
- Rhines, P. B. and W. R. Young. 1982a. Homogenization of potential vorticity in planetary gyres. *J. Fluid Mech.*, (in press).
- 1982b. A theory of the wind-driven circulation I. Mid-Ocean Gyres. *J. Mar. Res.*, *40*, (Supp.), 559-596.
- Stommel, H. 1948. The westward intensification of wind-driven ocean currents. *Trans. Amer. Geophys. Un.*, *29*, 202-206.
- 1965. *The Gulf Stream: A Physical and Dynamical Description*. University of California Press, Berkeley, and Cambridge University Press, London, 248 pp.
- Young, W. R. 1981. The vertical structure of the wind-driven circulation. Ph.D. thesis submitted to the Woods Hole Oceanographic Institution/Massachusetts Institute of Technology Joint Program in Oceanography and Ocean Engineering.